Polyketide reductases in defense-related parasorboside biosynthesis in Gerbera hybrida share processing strategies with microbial polyketide synthase systems

Zhu, Lingping

2022

Polyketide reductases in defense-related parasorboside biosynthesis in *Gerbera hybrida* share processing strategies with microbial polyketide synthase systems

Lingping Zhu (iD), **Milla Pietiäinen** (iD), **Juha Kontturi, Anna Turkkelin, Paula Elomaa** (iD) **and Teemu H. Teeri** (iD)

Department of Agricultural Sciences, Viikki Plant Science Centre, University of Helsinki, Helsinki, 00014 UH, Finland

Summary

Author for correspondence:
Teemu H. Teeri
Email: teemu.teeri@helsinki.fi

• Plant polyketides are well-known for their crucial functions in plants and their importance in the context of human health. They are synthesized by type III polyketide synthases (PKSs) and their final functional diversity is determined by post-PKS tailoring enzymes. *Gerbera hybrida* is rich in two defense-related polyketides: gerberin and parasorboside. Their synthesis is known to be initiated by GERBERA 2-PYRONE SYNTHASE 1 (G2PS1), but the polyketide reductases (PKRs) that determine their final structure have not yet been identified.
• We identified two PKR candidates in the pathway, GERBERA REDUCTASE 1 (GRED1) and GRED2. Gene expression and metabolite analysis of different gerbera tissues, cultivars, and transgenic gerbera plants, and *in vitro* enzyme assays, were performed for functional characterization of the enzymes.
• GRED1 and GRED2 catalyze the second reduction step in parasorboside biosynthesis. They reduce the proximal keto domain of the linear CoA bound intermediate before lactonization.
• We identified a crucial tailoring step in an important gerbera PKS pathway and show that plant polyketide biosynthesis shares processing strategies with fungi and bacteria. The two tailoring enzymes are recruited from the ancient sporopollenin biosynthetic pathway to a defense-related PKS pathway in gerbera. Our data provide an example of how plants recruit conserved genes to new functions in secondary metabolism that are important for environmental adaptation.

Introduction

Plant polyketides represent one of the largest groups of structurally and functionally diverse secondary metabolites. They exhibit a wide range of bioactivities and play important roles in a variety of biological and physiological functions, including pigmentation of flowers and fruits (anthocyanins), UV photoprotection (flavonoids), defense against pathogens and herbivores (e.g. stilbenes and 2-pyrones), and pollen development (sporopollenin; Austin & Noel, 2003; Grienenberger *et al.*, 2010; Koskela *et al.*, 2011; Deng *et al.*, 2014). Many of them are regarded as important medicinal compounds or potential novel therapeutics, given their antimicrobial, immunosuppressive, and anticancer properties (Stewart *et al.*, 2013; Lim *et al.*, 2016; Abe, 2020; Bisht *et al.*, 2021).

The core structures of the vast range of plant polyketides are biosynthesized by polyketide synthases (PKSs), which catalyze sequential decarboxylative condensations of an acyl-CoA starter with a malonyl-CoA extender, which is usually terminated by intramolecular cyclization (Austin & Noel, 2003; Morita *et al.*, 2019). Polyketide synthases are multifunctional enzymes derived from fatty acid synthase (FAS), and they fall into three groups

based on their architectural configuration (Austin & Noel, 2003). Fungal and bacterial polyketide biosynthesis relies mainly on large multi-domain type I and multi-enzyme type II PKSs. Besides essential functional domains or modules like acyl carrier proteins (ACP) and keto synthases (KS) for conducting starter loading and chain extension, they also contain optional tailoring domains or modules such as ketoreductases (KR), dehydratases (DH), enoyl reductases (ER) and cyclases (CYC; Hertweck, 2009; Neves *et al.*, 2021). Selective manipulations of growing polyketide chains performed by these tailoring proteins are one of the main factors contributing to the diversity of fungal and bacterial polyketides (Hertweck, 2009; Neves *et al.*, 2021). Type III PKSs, however, are simple homodimeric KSs that use a single active site to employ starter units and to perform iteratively decarboxylative condensations. The highly oxidated intermediates subsequently undergo cyclization by Claisen or aldol condensation, or by lactonization (Austin & Noel, 2003; Morita *et al.*, 2019). The processing of polyketide backbones to achieve the final structure and bioactivity is performed by post-PKS tailoring enzymes (Shimizu *et al.*, 2017; Morita *et al.*, 2019).

Type III PKSs are among the best-described enzymes in plants. So far, over 30 different plant PKS functions have been

characterized (Shimizu *et al.*, 2017). Diverse polyketide backbones are synthesized by using different starters, catalyzing different lengths of extension reactions, and terminating via different modes of intramolecular cyclization (Stewart *et al.*, 2013; Morita *et al.*, 2019). However, the post-PKS tailoring enzymes that determine the final functional diversity of plant polyketides are largely unknown.

Polyketide reductases (PKRs) are important accessory enzymes in many plant polyketide biosynthesis pathways, but only a few cases have been investigated in any detail. Chalcone reductase from Fabaceae, the three-dimensional structure of which has been established, specifically reduces a keto group of the nonaromatized coumaryl-trione intermediate, the immediate Claisen cyclized product of the chalcone synthase catalyzed coumaryl-tetraketide (Bomati *et al.*, 2005). In addition, the raspberry ketone/zingerone synthase (RZS) was found to reduce the PKS-synthesized diketide intermediate to raspberry ketone (Koeduka *et al.*, 2011). Polyketide reductases are always involved in the lactone-forming PKS pathways. The lactone-forming PKSs synthesize unreduced 2-pyrones in *in vitro* reactions, while *in planta* they cooperate with PKRs to make reduced lactones (e.g. gerberin and parasorboside in gerbera) or catalyze different types of cyclization (e.g. to naphthoquinones; Eckermann *et al.*, 1998; Jindaprasert *et al.*, 2008; Grienenberger *et al.*, 2010; Pietiäinen *et al.*, 2016). For example, the *Drosophyllum lusitanicum* PKS (DlHKS) was shown to produce a hexaketide 2-pyrone *in vitro*, and it has been suggested that it cooperates with an unknown PKR in plumbagin biosynthesis (Jindaprasert *et al.*, 2008). To date, the only two identified PKRs in the plant lactone-forming PKS pathways are the Arabidopsis TETRAKETIDE α-PYRONE REDUCTASE 1 (TKPR1) and TKPR2. They catalyze the reduction of the carbonyl group of the PKS-synthesized tetraketide intermediates to hydroxylated 2-pyrone compounds, important precursors of sporopollenin (Grienenberger *et al.*, 2010).

The ornamental plant gerbera (*Gerbera hybrida*) is rich in the polyketide-derived lactones gerberin, parasorboside and 4-hydroxy-5-methylcoumarin (HMC), which are mainly found in the tribe Mutisieae of Asteraceae (where *Gerbera* is located) and only sporadically in few other taxa (Murray, 1997; Koskela *et al.*, 2011). These compounds have been shown to play key role in defense against pathogens (Koskela *et al.*, 2011). They were also reported to be important bioactive compounds in some gerbera relatives (Nagumo *et al.*, 1989; He *et al.*, 2014), and they probably represent a major adaptive advantage of this branch of the Asteraceae family with respect to microbial attack and insect herbivores (Koskela *et al.*, 2011). The GERBERA 2-PYRONE SYNTHASE 1 (G2PS1) was originally identified due to its sequence similarity to chalcone synthases (Helariutta *et al.*, 1996). However, G2PS1 did not accept the bulky chalcone synthase starter molecule *p*-coumaroyl-CoA and it proved to be the first plant PKS described to use acetyl-CoA as a starter to synthesize a proposed intermediate, triacetolactone (TAL, 4-hydroxy-6-methyl-2-pyrone), in gerberin and parasorboside biosynthesis (Fig. 1), thus revealing a novel pathway in plant polyketide biosynthesis (Eckermann *et al.*, 1998). Later, we identified two homologues of G2PS1, G2PS2 and G2PS3, which initiate the biosynthesis of HMC by using the same substrates as G2PS1

but undergoing a longer chain extension (Pietiäinen *et al.*, 2016). More recently, we identified the anther-specific chalcone synthase-like enzymes GASCL1 and GASCL2 from gerbera (Kontturi *et al.*,
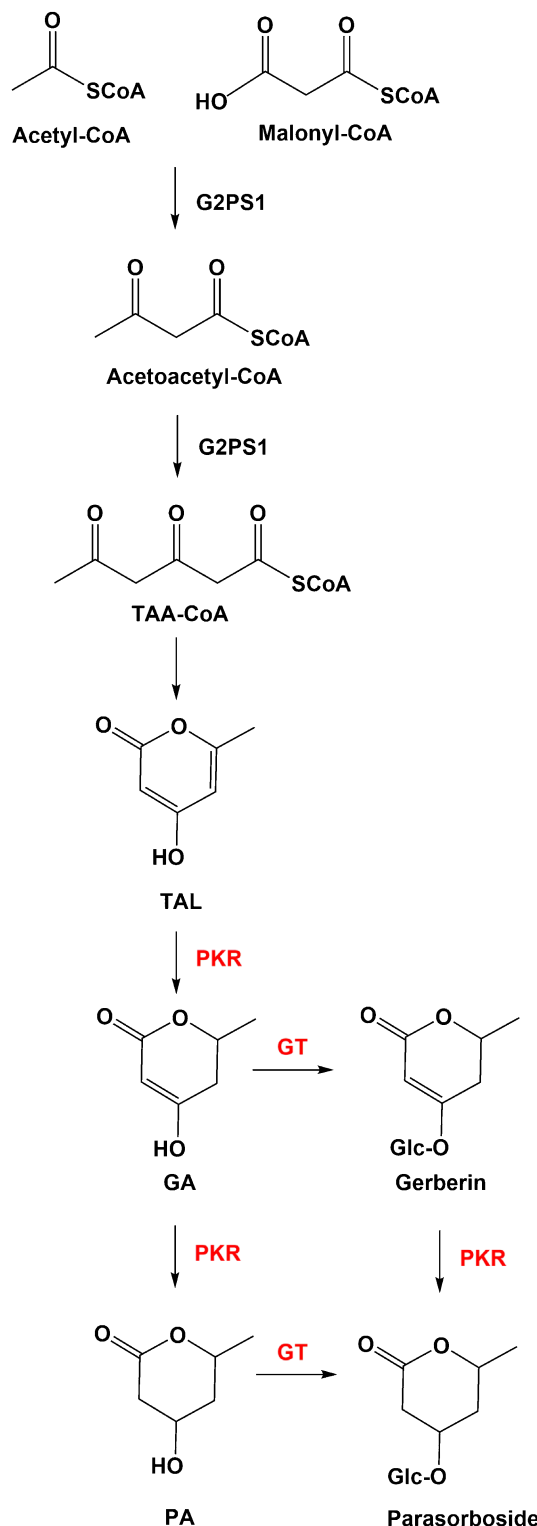
Fig. 1 Postulated biosynthetic pathway to gerberin and parasorboside. Unknown enzymes are in red. Conversion of TAA-CoA to TAL is probably nonenzymatic. CoA, coenzyme A; G2PS1, gerbera 2-pyrone synthase 1; GA, gerberin aglycone; GT, glucosyl transferase; PKR, polyketide reductase; TAA, triacetic acid; TAL, triacetolactone; PA, parasorboside aglycone.

2017). They are orthologues of the Arabidopsis PKSA and PKSB, respectively, and likewise utilize medium- or long-chain acyl-CoA starters to synthesize tetraketide 2-pyrone intermediates in sporopollenin biosynthesis (Kim *et al.*, 2010; Kontturi *et al.*, 2017). One or two thus-far-unknown PKRs have been proposed to reduce the 2-pyrone ring of TAL to get the aglycone form of gerberin and parasorboside (Fig. 1; Eckermann *et al.*, 1998). Similarly, it is thought that an unknown PKR processes the unreduced intermediate 4,7-dihydroxy-5-methylcoumarin into HMC in gerbera (Pietiäinen *et al.*, 2016).

In this study, we aimed to characterize the unknown PKRs in the PKS pathway leading to the synthesis of gerberin and parasorboside. We identified two TKPR2-like reductases encoded by *GERBERA REDUCTASE 1* (*GRED1*) and *GRED2* genes in gerbera. GRED1 is co-expressed with G2PS1, and GRED2 shows a high degree of sequence similarity with GRED1. We showed, by gene expression and metabolite analysis of different gerbera tissues, cultivars, and transgenic lines, and by *in vitro* enzyme assays, that the two reductases catalyze the second reduction step in parasorboside biosynthesis. However, GRED1 and GRED2 were shown to reduce not TAL, but a linear triketide intermediate before its lactonization, similar to the tailoring reactions in fungal and bacterial type I and type II PKS systems, indicating that the previously proposed pathway must be updated. Combined with our previous results (Zhu *et al.*, 2021), our data shows that these two enzymes were recruited from the ancient sporopollenin biosynthetic pathway to a defense-related PKS pathway. This demonstrates how plants recruit conserved genes to perform new functions within secondary metabolism, contributing to their environmental adaptation.

Materials and Methods

Plant material

Gerbera hybrida (*Gerbera jamesonii* Bolus ex Adlam × *Gerbera viridifolia* Schultz-Bip) cultivars 'Regina', 'President', 'Grizzly' and 'Pingpong' were obtained from Terra Nigra BV (De Kwakel, the Netherlands) and grown under conditions described previously (Ruokolainen *et al.*, 2010). Wild-type and transgenic gerbera plants were grown and multiplied *in vitro* as previously described (Elomaa & Teeri, 2001). Developmental stages of gerbera inflorescences have been described previously by Helariutta *et al.* (1993).

Identification and cloning of *GRED1* and *GRED2*

GERBERA REDUCTASE 1 (*GRED1*) was originally identified as the transcript with the highest expression correlation to *G2PS1* and was annotated as a 'reductase' in gerbera microarray data (Laitinen *et al.*, 2005). *GRED2* was further identified from the transcriptome data as a highly similar transcript to *GRED1*. *GRED1* and *GRED2* sequences (MW842919 and MW842920, respectively) were recovered in full length, and their coding sequences were amplified from the cultivar 'Regina' petal cDNA of development stage 6 (about half of the petals pigmented) with

gene-specific primers (Supporting Information Table S1). The polymerase chain reaction (PCR) products containing the full-length open reading frames of *GRED1* and *GRED2* with *attB* flanking sequences were cloned into the pDONR221 vector through the Gateway BP reaction (Katzen, 2007). The created entry clones were verified by sequencing.

RNAi and overexpression vector construction and gerbera transformation

The gene silencing constructs for *GRED1* and *GRED2* were generated by LR recombination between the entry clones and the Gateway binary vector pK7GWIWG2D(II) (Karimi *et al.*, 2002). The *GRED1* overexpression construct, under the control of the CaMV 35S promoter, was generated by LR recombination between the entry clone and the Gateway binary vector pK2GW7 (Karimi *et al.*, 2002). These expression constructs were electroporated into *Agrobacterium tumefaciens* strain C58C1(pGV2260) (Deblaere *et al.*, 1985) and subsequently transformed into gerbera cultivar 'Regina' as described previously by Elomaa & Teeri (2001).

Gene expression analysis with quantitative real-time polymerase chain reaction (qRT-PCR)

Gerbera tissue samples were collected from the cultivar 'Regina' for the determination of expression patterns of *G2PS1*, *GRED1* and *GRED2*. Petal, carpel, ovary, pappus, anther, receptacle, bract, and scape (the leafless inflorescence stem) samples were pooled samples corresponding to inflorescence development stages 2, 4, 6 and 8 (from emerging petals to fully open petals, see Helariutta *et al.*, 1993). Young leaves of 8–9 cm in length and fully expanded mature leaves of 37–38 cm in length were sampled separately. *In vitro* leaves were from 4–5 cm tall *in vitro* plants growing on rooting medium. For the determination of expression levels of *GRED1* and *GRED2* in different gerbera cultivars, fully expanded mature leaves were collected from the gerbera cultivars 'Regina', 'President', 'Pingpong' and 'Grizzly'. For the determination of *GRED1* and *GRED2* expression levels in gerbera transgenic lines, *in vitro* leaves were sampled from *GRED1* and *GRED2* RNAi transgenic lines, and mature leaf samples were collected from *GRED1* overexpression transgenic lines. Three biological replicates with three technical replicates from each sample were used for the expression analysis. Total RNA isolation was performed using a modified cetyltrimethylammonium bromide (CTAB) method, as described by Chang *et al.* (1993), followed by DNAase treatment using a NucleoSpin RNA Clean-up Mini Kit (740948.50; Macherey-Nagel, Düren, Germany) and verification in agarose gel that no DNA contamination remained. RNA quality and concentration was assessed using a Nanodrop Spectrophotometer (Thermo Scientific, Wilmington, NC, USA). One microgram of total RNA of each sample was applied in the synthesis of the first-strand cDNA, using a SuperScript III Reverse Transcriptase Kit (18 080 044; Invitrogen). Quantitative real-time polymerase chain reaction experiments were performed as described previously (Kontturi *et al.*, 2017) with primers listed in Table S1; melting curves of the

PCR products are shown in Fig. S1. Relative expression values were calculated using the $2^{-\triangle\triangle C_T}$ method (Livak & Schmittgen, 2001), and the gerbera housekeeping gene *GGAPDH* was applied as a reference.

Gerberin and parasorboside content analysis

Fresh gerbera tissues corresponding to the samples used for gene expression analysis were collected from 'Regina', 'Pingpong', 'President', 'Grizzly', transgenic *GRED1* and *GRED2* RNAi and overexpression lines, with two biological replicates for each sample. Fresh samples were ground into powder in liquid nitrogen and freeze-dried. Metabolites were extracted from the dried powders using a 20× volume of 100% methanol (20 µl methanol for each 1 mg dry sample) overnight at 4°C. Extracts were centrifuged (17 000 *g*, 5 min) and the supernatants were collected for thin-layer chromatography (TLC) analysis with ethyl acetate : formic acid : acetic acid : water (91 : 10 : 10 : 23, v/v) as mobile phase (Yrjönen *et al.*, 2002). Gerberin and parasorboside were visualized on the plates (TLC silica gel 60 F254; Merck, Darmstadt, Germany) after dipping in sulfuric acid : methanol (15 : 85, v/v) followed by heat treatment (120°C, 10 min; Ainasoja *et al.*, 2008). Photographs of the TLC plates were converted to 8-bit grayscale images with Fɪᴊɪ Imaɢᴇᴊ v.1.51, and the intensity of the spots corresponding to gerberin and parasorboside was measured to represent their amount. The percentage values of gerberin and parasorboside compared to the total amounts of the two compounds in each sample were calculated to represent the distribution between the two compounds.

Production of recombinant proteins

The recombinant G2PS1 was prepared in an *Escherichia coli* expression system, constructed as described previously (Pietiäinen *et al.*, 2016). Recombinant GRED1 and GRED2 were prepared in a plant expression system. The coding sequences of *GRED1* and *GRED2* were cloned into the plant expression vector pEAQ-HT-DEST2 (Sainsbury *et al.*, 2009) and electroporated into the *A. tumefaciens* strain C58C1(pGV2260) (Deblaere *et al.*, 1985). The recombinant proteins were transiently expressed in leaves of 6-wk-old *Nicotiana benthamiana* plants by agroinfiltration as described previously (Bashandy *et al.*, 2015). The infiltrated leaves were sampled 3 d later, and soluble proteins were extracted from the leaf samples using cold extraction buffer (degassed 100 mM Tris–HCl, pH 7.5) supplemented with 0.2% β-mercaptoethanol and complete Mini EDTA free protease inhibitor cocktail (04693159001; Roche), homogenized on ice, then centrifuged for 17 000 *g*, 10 min at 4°C. Small molecules were removed with PD MiniTrap G-25 columns (28 918 007; GE Healthcare, Freiburg, Germany) before performing enzyme assays.

Enzyme assays

Enzyme assays for the reductases were conducted in a 100 µl reaction volume containing 100 mM HEPES-KOH buffer (pH 6.0), 1 mM NADPH (N2385; Sigma), 15–20 µg of tobacco protein extract containing recombinant GRED1 or GRED2, and 10 µl of substrate, incubated at 30°C for 1 h and terminated by adding 20 µl acetic acid. As candidate substrates for GRED1 and GRED2, TAL (H43415; Sigma) and gerberin aglycone (309 680; Sigma) were prepared as 1 mg ml⁻¹ stock in 100 mM HEPES-KOH buffer (pH 6.0). In addition to TAL and gerberin aglycone, a metabolite mixture was prepared from methanol extracts of gerbera leaves. Among other compounds, these extracts are rich in gerberin and parasorboside (Eckermann *et al.*, 1998). Two 100 µl samples of methanol extracts were evaporated to dryness. One sample was dissolved in 40 µl HEPES-KOH buffer (pH 6.0) and was directly applied as substrate in the enzyme assays. The other sample was treated with β-glucosidase to produce aglycone substrates for the enzymatic assays. For this purpose, the sample was dissolved in 300 µl of 100 mM Na-acetate buffer (pH 5.0) containing 2 mg β-glucosidase (49 290; Sigma) and incubated for 3 h at 37°C. The reaction was stopped with 10 µl 4 M HCl and extracted twice with 350 µl ethyl acetate, evaporated to dryness in a vacuum centrifuge, and then dissolved in 40 µl 100 mM HEPES-KOH buffer (pH 6.0).

The products of enzyme assays with the candidate substrates were extracted, after stopping, twice with 200 µl ethyl acetate and evaporated to dryness. The dry products were dissolved in 10 µl methanol and analyzed with silica TLC with methanol : dichloromethane (15 : 85, v/v) as mobile phase. Consumption of TAL, gerberin aglycone, or gerberin was visualized under UV light at 252 nm.

The radiometric enzyme assays were conducted in 100 µl volume of 100 mM HEPES-KOH buffer (pH 6.0) containing 10–15 µg of recombinant G2PS1 protein, 10 µM acetoacetyl-CoA (A1625; Sigma) and 10 µM [2-¹⁴C]-labeled malonyl-CoA (NEC612; PerkinElmer, Boston, MA, USA). After 30 min incubation at 30°C, 15–20 µg of tobacco protein extract containing recombinant GRED1 or GRED2 and 1 mM NADPH were added to the reaction, and the incubation was continued for another 2 h. The reactions were stopped by adding 30 µl of acetic acid. The products were extracted twice with 200 µl ethyl acetate and evaporated to dryness. The dry products were dissolved in 10 µl methanol and applied to silica TLC with ethyl acetate : methanol : water (100 : 16.5 : 13.5, v/v) as mobile phase. The radio-labelled products were visualized by 10-d exposure to high-performance chemiluminescence film (28 906 835; GE Healthcare).

Assays with the linear triketide substrate analog methyl 3,5-dioxohexanoate (abcr, Karlsruhe, Germany) were conducted in 100 µl of 100 mM potassium phosphate buffer (pH 6.6) containing 10 µl (5–10 µg) tobacco protein extract containing GRED1 or GRED2, 0.1 mM NADPH and 0.63 mM substrate. After the consumption of NADPH, absorbance at 340 nm was monitored.

Results

Identification and cloning of *GRED1* and *GRED2*

Previously, *G2PS1* was identified and shown to encode the committed PKS which catalyzes the first step in gerberin and

parasorboside biosynthesis in *G. hybrida* (Helariutta *et al.*, 1996; Eckermann *et al.*, 1998). To identify the accessory tailoring enzymes in the pathway, we searched for reductase-encoding genes that share a similar expression pattern with G2PS1 from our early transcriptome data (Laitinen *et al.*, 2005). By conducting Pearson correlation analysis, we identified a transcript containing the full-length coding sequence of a short-chain dehydrogenase/reductase (SDR) that was coexpressed with *G2PS1*, and we named it *GERBERA REDUCTASE 1* (*GRED1*). In the transcriptome data, we discovered another transcript encoding a similar SDR gene that shared 85% nucleotide sequence identity with *GRED1*, and we named it *GRED2*. The two genes were considered as potential candidate genes encoding reductases in the gerberin and parasorboside biosynthetic pathway. The full-length coding sequences of *GRED1* and *GRED2* were amplified from gerbera petal cDNA. Both *GRED1* and *GRED2* contain a 960-bp open reading frame encoding polypeptides of 320 amino acids, sharing 84% amino acid sequence identity with each other. They are both similar (67% and 65% amino acid sequence identity, respectively) to the Arabidopsis tetraketide α-pyrone reductase encoding gene *TKPR2* (Zhu *et al.*, 2021).

GRED1 and *GRED2* show diverse expression patterns in gerbera

In Arabidopsis, *AtTKPR2* is a single-copy gene and is expressed specifically in anthers (Grienenberger *et al.*, 2010). Preliminary analysis of the transcriptome data indicated that *GRED1* and *GRED2* are not anther specific and *GRED1* is co-expressed with the widely expressed *G2PS1* gene. We determined the spatial expression profiles of *GRED1*, *GRED2*, and *G2PS1* using qRT-PCR. In 12 selected vegetative and reproductive tissues of the cultivar 'Regina', our results showed that *GRED1* and *GRED2* have diverse expression patterns, and neither was restricted to the anthers (Fig. 2a). The *GRED1* expression profile across the tissues is highly similar to that of *G2PS1*, and it shows the highest expression in *in vitro* leaf, carpel, and ovary tissues, and somewhat lower expression in anthers and roots (Fig. 2a). *GRED2* expression, however, is highest in the receptacle, scape, and *in vitro* leaves (Fig. 2a). The expression of both *GRED1* and *GRED2* was relatively high in *in vitro* leaves but was lower in young and mature leaves (Fig. 2a).

The distribution of gerberin and parasorboside in gerbera tissues

To explore whether the expression levels of candidate genes *GRED1* and *GRED2* are correlated with the biosynthesis of gerberin and parasorboside, we analyzed the spatial distribution of the two compounds in the gerbera tissues corresponding to those used for the gene expression analysis. Using TLC followed by sulfuric acid staining to analyze the metabolites (Yrjönen *et al.*, 2002), gerberin and parasorboside could be separated and visualized. The grayscale intensities of spots corresponding to the two compounds in photographed TLC plates were determined to represent the distribution of the compounds in the samples in a semiquantitative way. The metabolite analysis showed that gerberin and parasorboside accumulated in nearly all gerbera tissues; however, they were observed to be present at very low concentrations in anthers and roots, where *G2PS1* (and *GRED1*) also showed the lowest expression levels (Fig. 2b). Moreover, the relative distribution of gerberin and parasorboside showed variation between the tissues (Fig. 2b,c). Parasorboside was preferentially accumulated in the young and *in vitro* leaves, receptacle, root, and scape tissues, while gerberin accumulated preferentially in bract, carpel, anther, pappus, ovary, and petal tissues (Fig. 2b,c). Distinct gerberin and parasorboside distribution patterns were observed between leaves of different stages (Fig. 2b,c). The *in vitro* leaves were shown to almost exclusively synthesize parasorboside, young leaves to produce more parasorboside than gerberin, and the mature leaves to accumulate more gerberin than parasorboside (Fig. 2b,c).

The distribution of gerberin and parasorboside in gerbera cultivars

We determined in an earlier study (Ainasoja *et al.*, 2008) that while all gerbera cultivars produce gerberin and parasorboside in leaves and flowers, the ratio of these metabolites varies. To further explore the relationship between *GRED1* and *GRED2* expression and gerberin and parasorboside accumulation, we investigated the expression levels of *GRED1* and *GRED2* and the contents of the two compounds in mature leaves from gerbera cultivars 'Regina', 'President', 'Pingpong' and 'Grizzly'. The expression levels of *GRED1* and *GRED2* varied between the cultivars (Fig. 2d). Compared with 'Regina', *GRED1* was more strongly expressed in 'Pingpong' and 'Grizzly', while *GRED2* showed higher expression levels in 'President' and 'Pingpong' (Fig. 2d). The gerberin and parasorboside content in mature leaves from these cultivars were analyzed with TLC. Cultivars 'President', 'Pingpong' and 'Grizzly' accumulated parasorboside preferentially, in contrast to 'Regina' that accumulated gerberin preferentially (Fig. 2e,f).

Overexpression of *GRED1* in gerbera results in an increase in parasorboside accumulation at the expense of gerberin in transgenic gerbera leaves

To investigate the role of *GRED1* and *GRED2* in gerberin/parasorboside biosynthesis, we tried to produce transgenic gerbera lines overexpressing *GRED1* and *GRED2*. We successfully obtained three transgenic lines transformed with the *GRED1* overexpression construct but failed to get correct lines with the *GRED2* construct. Two of the three transgenic lines, TR2 and TR3, showed significant overexpression of *GRED1* in leaves, while *GRED1* expression was reduced in TR1, a likely co-suppression effect (Fig. 3a). In all three lines, expression of *GRED2* was lower than in the wild-type (Fig. 3a). We next analyzed the changes in gerberin and parasorboside distribution in these transgenic lines. Compared with the gerberin and parasorboside content in the mature leaves of the wild-type, there was an
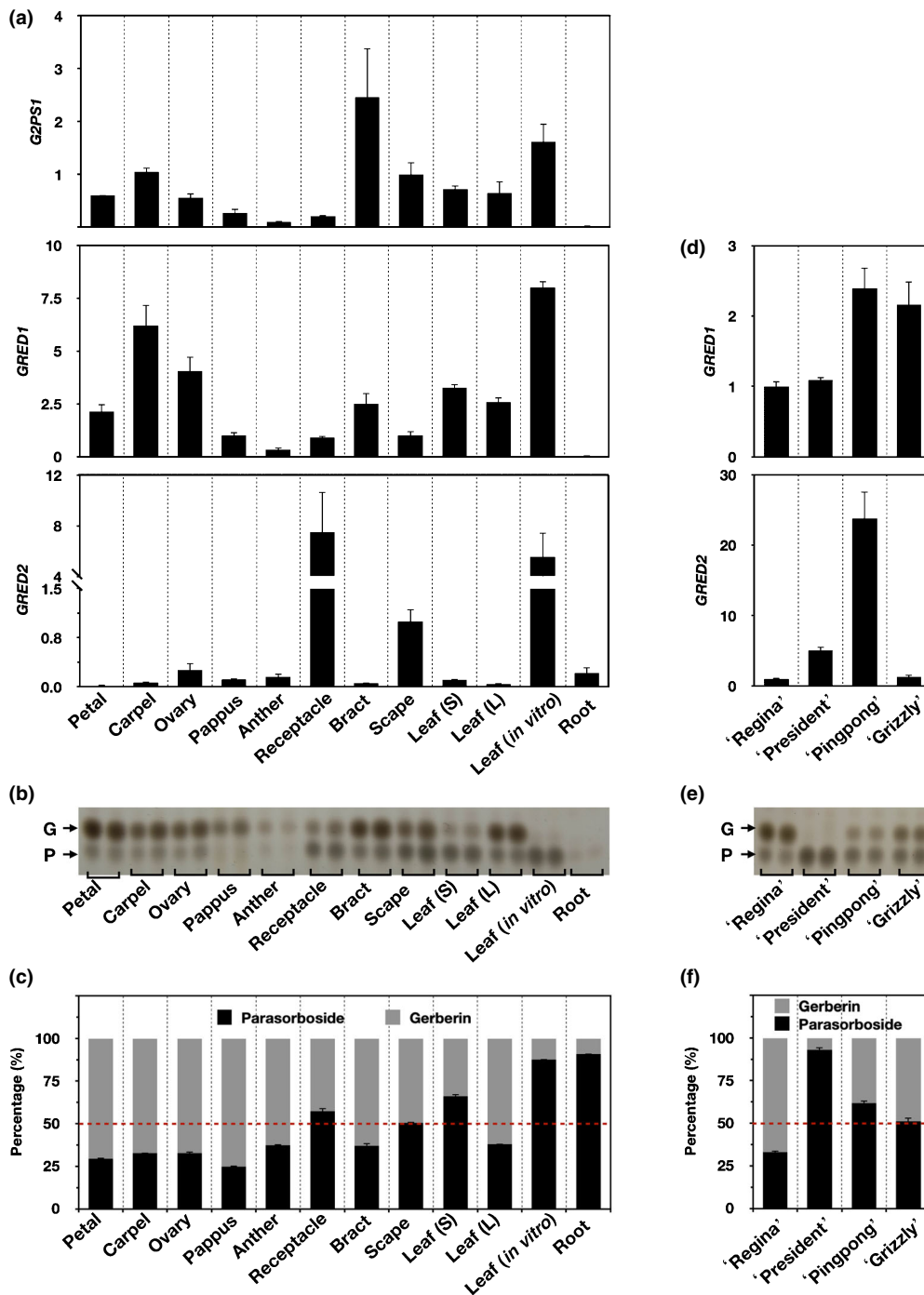
Fig. 2 Expression patterns of *G2PS1*, *GRED1* and *GRED2*, and distribution of gerberin and parasorboside in different gerbera tissues and cultivars. (a) Quantitative real-time polymerase chain reaction analysis of relative *G2PS1*, *GRED1* and *GRED2* expression levels in a gerbera tissue series. Expression was calculated using the $2^{-\triangle\triangle C_T}$ method and is represented relative to expression levels in 'Scape', which was set at 1. Error bars (SE) were calculated from three biological replicates. Tissue series were from cv. 'Regina'. Leaf (*in vitro*), leaves from 4–5 cm tall *in vitro* plants; Leaf (L), fully expanded mature leaves; Leaf (S), young leaves of 8–9 cm in length. (b) Thin-layer chromatography (TLC) analysis of methanol extracts from gerbera tissue series. G, gerberin; P, parasorboside. (c) Distribution of gerberin and parasorboside in the gerbera tissue series. Grayscale values for the spots corresponding to gerberin and parasorboside on the TLC image were measured to represent their amounts, and their proportions were calculated to represent the distribution of the two compounds. Error bars (SE) are calculated from two biological replicates. Red dashes represent the 50% level. (d) Quantitative real-time polymerase chain reaction analysis of relative *GRED1* and *GRED2* expression levels in fully expanded mature leaves of gerbera cultivars. Expression was calculated as described for (a) and is represented relative to expression levels in 'Regina', which was set at 1. Error bars (SE) were calculated from three biological replicates. (e) Thin-layer chromatography analysis of methanol extracts from fully expanded mature leaves of gerbera cultivars. (f) Distribution of gerberin and parasorboside in the cultivars. Error bars (SE) are calculated from two biological replicates.
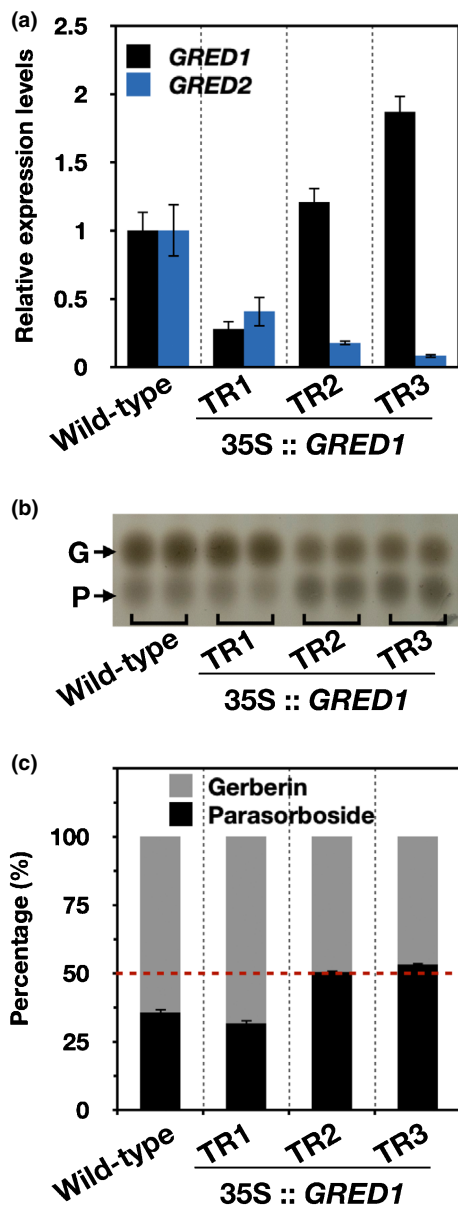
Fig. 3 Expression and gerberin and parasorboside content analysis of transgenic gerbera *GRED1* overexpression lines. (a) Quantitative real-time polymerase chain reaction analysis of relative *GRED1* and *GRED2* expression levels in fully expanded mature leaves of wild-type and gerbera *GRED1* overexpression lines. Expression was calculated using the $2^{-\triangle\triangle C_T}$ method and is represented relative to expression levels in the wild-type, which was set at 1. Error bars (SE) were calculated from three biological replicates. (b) Thin-layer chromatography (TLC) analysis of methanol extracts from fully expanded mature leaves of wild-type and gerbera *GRED1* overexpression lines. G, gerberin; P, parasorboside. (c) Distribution of gerberin and parasorboside in fully expanded mature leaves of wild-type and gerbera *GRED1* overexpression lines. Grayscale values for the spots corresponding to gerberin and parasorboside on the TLC image were measured to represent their amounts, and their proportions were calculated to represent the distribution of the two compounds. Error bars (SE) were calculated from two biological replicates. Red dashes represent the 50% level.

increase in parasorboside content and a decrease in gerberin content in the leaves of transformants TR2 and TR3, where *GRED1* was overexpressed (Fig. 3a–c).

Decreased parasorboside accumulation with increased gerberin accumulation in gerbera *GRED1* and *GRED2* downregulation lines

To further clarify the functions of *GRED1* and *GRED2* in gerberin and parasorboside biosynthesis, we applied a double-stranded RNA interference (RNAi) vector to produce *GRED1* and *GRED2* downregulated gerbera transgenic lines. The high degree of nucleotide sequence similarity of *GRED1* and *GRED2* resulted in cross-downregulation of both genes in many transgenic plants (Fig. 4a). The expression of *GRED1* and *GRED2* in *in vitro* leaves of these transgenic lines was analyzed, and we identified several lines that displayed suppression of *GRED1* and/or *GRED2* expression (Fig. 4a).

The *in vitro* leaves of nontransgenic cultivar 'Regina' accumulate parasorboside almost exclusively (Fig. 4b,c). However, the two severely *GRED1/2* double downregulated lines (*GRED2* RNAi TR8 and TR12) produced gerberin almost exclusively (Fig. 4b,c). This indicates that either GRED1 or GRED2 expression is necessary for the biosynthesis to proceed towards parasorboside. When both are missing, gerberin accumulates instead.

Enzymatic activity of GRED1 and GRED2

According to the previously proposed pathway (Eckermann *et al.*, 1998; Fig. 1), TAL could be the potential substrate for the first PKR, and gerberin aglycone (or gerberin) the potential substrate for the second PKR on the pathway to the glucosides gerberin and parasorboside. To investigate the enzymatic activity of GRED1 and GRED2, we conducted *in vitro* enzyme assays to test these potential substrates. Besides the commercially available TAL and gerberin aglycone, we also tested gerbera native metabolites prepared from leaf methanol extracts and their deglycosylated forms prepared by β-glucosidase treatment. Thin-layer chromatography analysis of the enzyme assay products showed that there is no detectable consumption of TAL, gerberin, or gerberin aglycone in reactions containing the cofactor NADPH and heterologously expressed GRED1 or GRED2, compared with control reactions that contained *N. benthamiana* crude proteins only (Fig. 5a). This suggests that the substrates for GRED1 or GRED2 might not be the previously proposed TAL, gerberin aglycone or gerberin. Instead, the true substrate could be a thus-far-unrecognized intermediate in the pathway.

To explore this possibility, we reconstructed the biosynthetic pathway *in vitro*, by providing acetoacetyl-CoA, [2-^{14}C]-labeled malonyl-CoA, and heterologously expressed G2PS1 in the enzyme assays to produce radiolabeled potential intermediate substrates, and then adding NADPH and GRED1 or GRED2. The generated products were extracted with ethyl acetate and fractionated by TLC, and the radiolabeled products were visualized by exposure to photographic film. The result showed that G2PS1 synthesizes TAL, consistent with previously reported results (Eckermann *et al.*, 1998). However, a new compound running slower than TAL was generated at the expense of TAL when providing the cofactor NADPH and GRED1 or GRED2 separately (or together) in the assays (Fig. 5b). The new
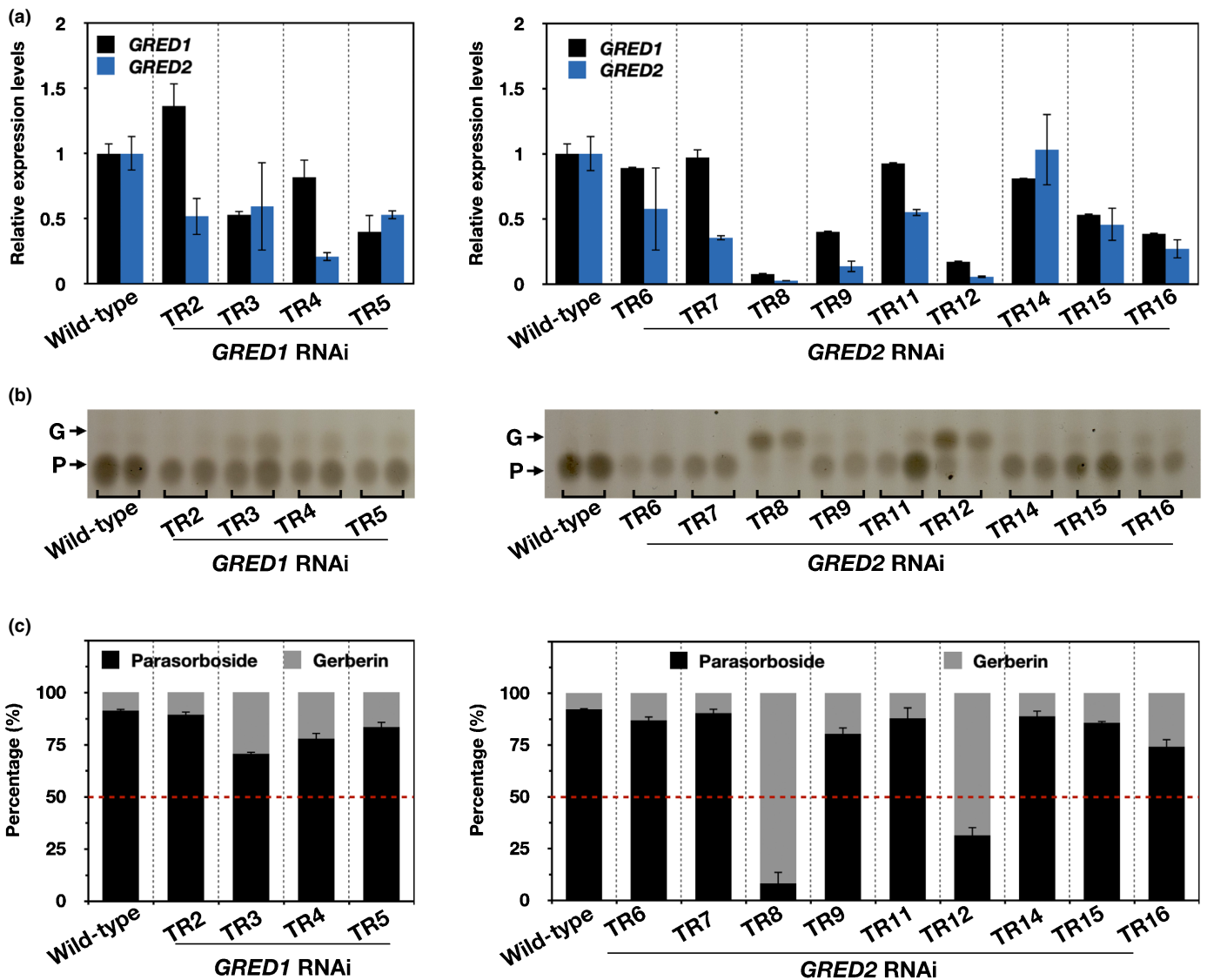
Fig. 4 Expression and gerberin and parasorboside content analysis of transgenic gerbera *GRED1* and *GRED2* RNAi downregulated lines. (a) Quantitative real-time polymerase chain reaction analysis of relative *GRED1* and *GRED2* expression levels in *in vitro* leaves of wild type, *GRED1* RNAi and *GRED2* RNAi lines. Expression was calculated using the $2^{-\triangle\triangle C_T}$ method and is represented relative to expression levels in the wild-type, which was set at 1. Error bars (SE) were calculated from three biological replicates. (b) Thin-layer chromatography (TLC) analysis of methanol extracts from *in vitro* leaves of wild-type, *GRED1* RNAi and *GRED2* RNAi lines. G, gerberin; P, parasorboside. (c) Distribution of gerberin and parasorboside in *in vitro* leaves of wild-type, *GRED1* RNAi and *GRED2* RNAi lines. Grayscale values for the spots corresponding to gerberin and parasorboside on the TLC image were measured to represent their amounts, and their proportions were calculated to represent the distribution of the two compounds. Error bars (SE) were calculated from two biological replicates. Red dashes represent the 50% level.

compound was not formed without NADPH or either of the two reductases (Fig. 5b), indicating that it was a reduced compound made by GRED1 and GRED2. Both reductases functioned with equal efficiencies and produced a compound with identical mobility in TLC (Fig. 5b).

As the product of the radiometric enzyme assay remained unknown, we tested whether methyl 3,5-dioxohexanoate could be reduced by GRED1 or GRED2. This molecule is a methyl ester of the linear triketide, resembling the CoA thioester of the G2PS1 product before its lactonization. Both GRED1 and GRED2 showed NADPH consumption when this substrate was provided (Table 1; Fig. S2).

Discussion

GRED1 and GRED2 are the PKRs necessary for parasorboside biosynthesis

Two closely related glucosidic lactones, gerberin and parasorboside, are known to be synthesized through a shared PKS pathway initiated by G2PS1, but the PKRs determining their final structure have remained unknown. In this work, we identified two PKRs that are important for parasorboside biosynthesis, the SDR superfamily reductases GRED1 and GRED2. *GRED1* was identified by its co-expression pattern with *G2PS1*, and *GRED2* was
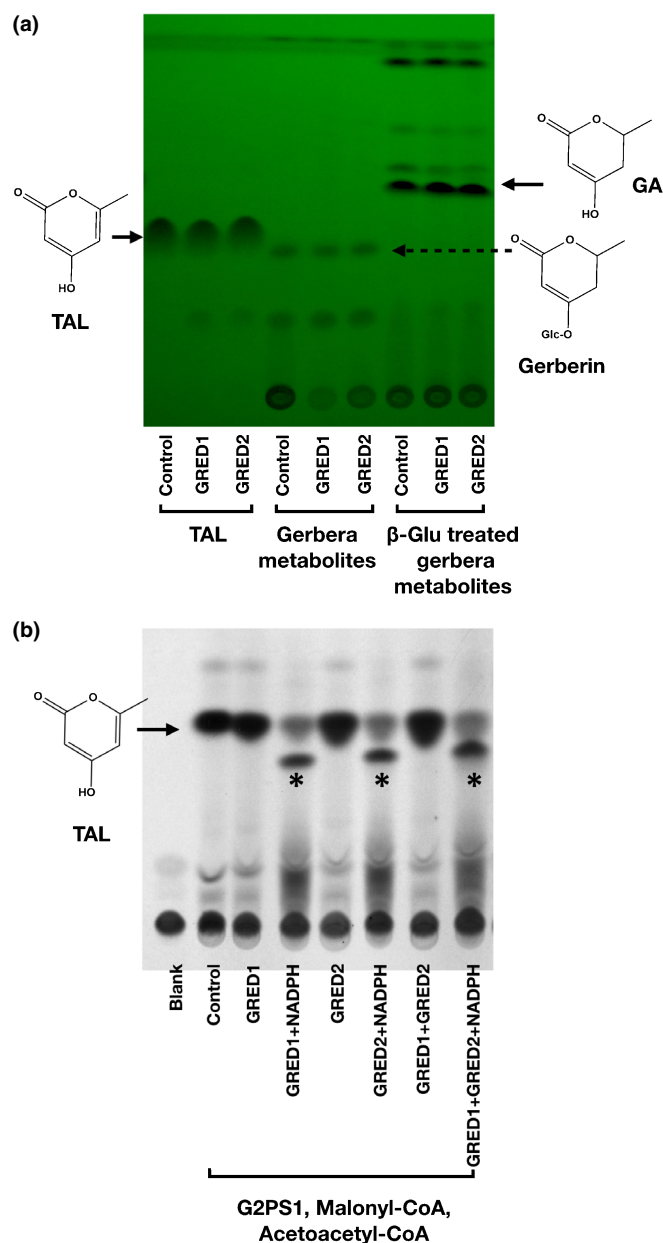
Fig. 5 Thin-layer chromatography (TLC) analysis of *in vitro* reaction products of GRED1 and GRED2. (a) Comparison of consumption of proposed substrates in *in vitro* reaction of GRED1 and GRED2. Commercial 4-hydroxy-6-methyl-2-pyrone (TAL), gerbera methanol extracts rich in gerberin, and β-glucosidase treated gerbera methanol extracts that are rich in gerberin aglycone were tested as substrates. Tobacco protein extracts containing recombinant GRED1 or GRED2 were applied, and tobacco protein extracts from noninfiltrated tobacco leaves served as control. 1 mM NADPH was applied in all reactions. (b) Comparison of product profiles in *in vitro* reactions of G2PS1 together with (and without) GRED1 or GRED2. G2PS1 and common substrates [2-¹⁴C] malonyl-CoA and acetoacetyl-CoA were applied in all reactions; GRED1, GRED2 and NADPH were applied in marked reactions, forming a new compound (*); tobacco protein extracts from non-infiltrated tobacco leaves were included in the control reaction; 'Blank' refers to a control reaction that was stopped before adding the enzymes.

Table 1 Reduction of methyl 3,5-dioxohexanoate by GRED1 and GRED2.

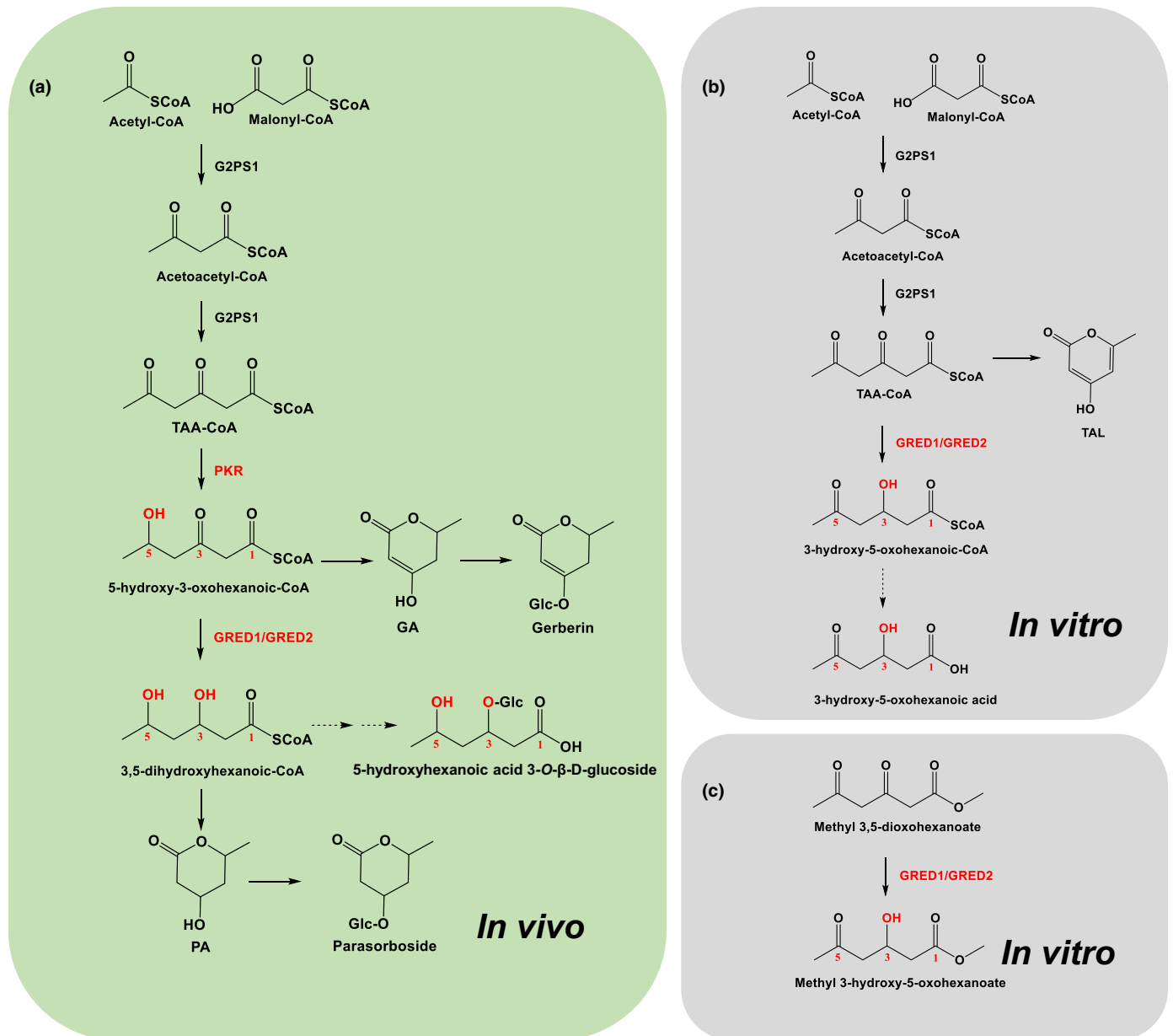|	NADPH consumption	Relative activity
Blank (no extract)	0.051	–
Control (tobacco extract)	0.091	1
Tobacco extract containing GRED1	0.154	2.6
Tobacco extract containing GRED2	0.250	5.0

NADPH consumption was measured by following the decrease in absorbance at 340 nm for 30 min.

distribution between gerberin and parasorboside in gerbera. We showed that the pathway preferentially synthesizes parasorboside in tissues and cultivars exhibiting high *GRED1* or *GRED2* expression, and tend to produce more gerberin in tissues and transgenic lines exhibiting low *GRED1* and *GRED2* expression. The strongest support came from transgenic gerbera lines in which downregulation of both *GRED1* and *GRED2* together abolished parasorboside accumulation, and only gerberin was made. These data suggest that GRED1 and GRED2 are the key branch-point PKRs in gerberin/parasorboside biosynthesis. In particular, they catalyze the second reduction step in the pathway, since no correlated changes in the total content of the two compounds were observed in the transgenic (upregulated or downregulated) lines.

GRED1 and GRED2 reduce the proximal keto domain of the linear triketide intermediate before lactonization

In the previously proposed gerberin/parasorboside biosynthetic pathway, it was proposed that one or two reductions in the 2-pyrone ring of TAL, performed by one or two missing PKRs, were required for the formation of gerberin and parasorboside (Eckermann *et al.*, 1998; Fig. 1). However, TAL, gerberin aglycone or gerberin could not be reduced by GRED1 or GRED2 in our *in vitro* enzyme assays. This suggested that none of these lactones is the substrate for GRED1 or GRED2, and our previously proposed pathway needs an update. Another possibility is that the PKRs act on linear intermediates before their lactonization. This does not seem to take place at the diketide intermediate. Although the unreduced diketide acetoacetyl-CoA is readily extended by G2PS1, 3-hyroxybutyryl-CoA and crotonyl-CoA (reduced diketides) are not (Eckermann *et al.*, 1998). The remaining linear intermediate is the triketide 3,5-dioxohexanoic-CoA, where the distal keto group is first reduced to produce 5-hydroxy-3-oxohexanoic-CoA. The proximal group is then reduced by the second PKR (GRED1 or GRED2) to generate 3,5-dihydroxyhexanoic-CoA (Fig. 6a). These reduced linear intermediates are subsequently lactonized to gerberin aglycone and parasorboside aglycone, respectively (Fig. 6a). In this scenario, TAL is a derailment product rather than an intermediate in gerberin and parasorboside biosynthesis.

Similar reactions have been reported in other PKS pathways. An unidentified KR was shown to be involved in 6-

distinguished through its high nucleotide sequence identity with *GRED1*. Expression and metabolite analysis indicated that GRED1 and GRED2 might be associated with the differences in

Fig. 6 Updated *in vivo* and *in vitro* biosynthetic pathways to gerberin and parasorboside. (a) Our results indicate that reduction of the triketide backbone leading to gerberin and parasorboside takes place before lactonization; this idea is supported by the presence of the reduced linear form as a glucoside in gerbera tissues. (b, c) Consequently, the *in vitro* products of GRED1 and GRED2 would be 3-hydroxy derivatives of the substrates. G2PS1, gerbera 2-pyrone synthase 1; GA, gerberin aglycone; PA, parasorboside aglycone; PKR, polyketide reductase; TAA-CoA, triacetic acid-CoA; TAL, triacetolactone. Polyketide reductases and proposed reduced substituents are marked in red. Dashed arrows refer to speculated reactions.

hydroxymellein biosynthesis in carrot, reducing the distal keto group of a triketide intermediate to form a 5-hydroxy-3-oxohexanoic-CoA intermediate, and TAL was produced as a derailment product when NADPH was absent (Kurosaki *et al.*, 2002). This KR catalyzes a similar reaction to the proposed first (as yet uncharacterized) PKR catalyzed reaction in gerberin biosynthesis (Fig. 6a). In 6-methylsalicylic acid (6-MSA) biosynthesis in fungus, the triketide-CoA was lactonized to TAL instead of the 3-hydroxy intermediate, when the KR domain of the type I PKS was mutated or blocked by the absence of NADPH (Scott *et al.*, 1974; Campuzano & Shoolingin-Jordan, 1998). This KR

catalyzes the same reaction as GRED1 and GRED2 in the updated parasorboside biosynthesis scheme and, furthermore, GRED1 and GRED2 readily reduce the linear triketide substrate analog methyl 3,5-dioxohexanoate (Fig. 6). Recently, 5-hydroxyhexanoic acid 3-*O*-β-D-glucoside was identified in and isolated from gerbera leaves, and it was suggested that it is synthesized through the shared gerberin/parasorboside biosynthetic pathway (Mascellani *et al.*, 2021). This finding supports our updated pathway and suggests that PKRs do indeed act on the linear triketide before lactonization, and the reduced triketide either lactonizes to parasorboside aglycone or is released and

glucosylated, converting to the 5-hydroxyhexanoic acid 3-*O*-β-D-glucoside (Fig. 6a). Many gerbera cultivars are rich in both gerberin and parasorboside, and both gerberin aglycone and parasorboside aglycone accumulate in the plant under stress (Koskela *et al.*, 2011), but neither TAL nor its glucoside has ever been detected in gerbera.

The updated pathway suggests that all PKS pathways share similar processing strategies

In bacteria and fungi, functional modules like KR, DH, ER and CYC are commonly present in type I and II PKS systems. They act on the linear intermediates and are required for the correct region-specific cyclization of the growing chain (Fischbach & Walsh, 2006; Hertweck, 2009; Neves *et al.*, 2021). The production of lactones as derailment products has been observed in many type I and II PKS initiated pathways when the KR was missing or blocked, such as in the type I PKS catalyzed 6-MSA biosynthesis (Campuzano & Shoolingin-Jordan, 1998) or type II PKS initiated actinorhodin biosynthesis, in which an SDR type KR is involved (Hadfield *et al.*, 2004). The lactonization of linear polyketide thioesters into 2-pyrones is in fact a spontaneous reaction (Light *et al.*, 1966; Springob *et al.*, 2007). This explains why a lactone is frequently produced as a derailment product in PKS pathways when the system is absent of tailoring enzyme functions. Polyketide reductases acting on linear intermediates before cyclization in the updated gerberin/parasorboside pathway highly resemble the tailoring reactions performed by optional KR subunits in type I and II PKS systems. Similar reactions are thought to occur in many other lactone-forming type III PKSs. For instance, unknown PKRs are supposed to be involved in the *Plumbago* PKS or *Drosophyllum* HKS initiated natural polyketide biosynthesis pathways (Springob *et al.*, 2007; Jindaprasert *et al.*, 2008). These plant PKSs were again shown to make lactones *in vitro* instead of producing the expected intermediates in the original plants. Clearly, the accessory PKRs in the lactone forming PKS initiated pathways play a crucial function in stabilizing the linear intermediates and preventing them from unspecific cyclization during their biosynthesis. The similarity in tailoring reactions among the type I, II and III PKS pathways is also supported by observations of the first plant polyketide CYC, olivetolic cyclase (OAC), which is involved in cannabinoid biosynthesis in *Cannabis sativa* (Gagne *et al.*, 2012). Olivetolic cyclase is structurally similar to type II PKS associated CYC and catalyzes cyclization of the linear tetraketide intermediate to olivetolic acid, instead of the derailment products olivetol and 2-pyrones, a similar reaction to that which occurs in type II PKS system catalyzed pathways (Gagne *et al.*, 2012).

GRED1 and GRED2 were recruited from the conserved sporopollenin biosynthesis pathway to defense-related polyketide biosynthesis

GRED1 and *GRED2* are both close orthologues of the Arabidopsis *TKPR2*, which encodes one of the two anther-specific PKRs involved in sporopollenin biosynthesis. As a major structural element of pollen walls, sporopollenin is crucial for the reproductive success of land plants (Wallace *et al.*, 2011; Quilichini *et al.*, 2015). Sporopollenin has been shown to be synthesized through an ancient PKS pathway constructed from a set of functionally conserved enzymes (Kim & Douglas, 2013). In Arabidopsis, two PKRs, the predominant AtTKPR1 and the minor AtTKPR2, reduce the PKS synthesized tetraketide 2-pyrones into hydroxylated 2-pyrones, which are important sporopollenin precursors (Grienenberger *et al.*, 2010). Gerbera has a single *TKPR1* orthologue (*GTKPR1*) that is anther-specific (Zhu *et al.*, 2021), and two non-anther-specific *AtTKPR2* orthologues, *GRED1* and *GRED2*, which are described here. In our previous work we showed that while GTKPR1 is the predominant PKR in sporopollenin biosynthesis (as AtTKPR1 is in Arabidopsis), the *TKPR2* othologues *GRED1* and *GRED2* have maintained not only expression in the tapetum of anthers but also involvement in pollen wall biosynthesis to some extent (Zhu *et al.*, 2021). However, the dramatically expanded expression patterns of *GRED1* and *GRED2* indicated that they have probably been recruited to novel functions out of sporopollenin biosynthesis, and in this study we show what these functions are. During evolution, GRED1 and GRED2 have been recruited from the ancient sporopollenin biosynthesis pathway to the defense-related polyketide biosynthesis pathway in gerbera.

Plants have adapted to changing environments and biotic challenges by producing a wide range of secondary metabolites. However, secondary metabolism associated protein folds are restricted (Weng *et al.*, 2012). Gene duplication is believed to be the driver of metabolic innovation (Moghe & Last, 2015). The diversification of plant secondary metabolism is believed to be an evolutionary result of gene duplication events and subsequently functional divergence events (Moghe & Last, 2015). This mechanism is well reflected in the evolution of plant polyketide biosynthesis. Plant PKSs have shared protein folds but synthesize diverse polyketide backbones, relying on slight variations of their catalytic cavity. They have been shown to be derived from FAS and have acquired functional diversity through gene duplication and mutation events (Jenke-Kodama *et al.*, 2008; Xie *et al.*, 2016; Yonekura-Sakakibara *et al.*, 2019). The sporopollenin biosynthesis associated PKSA/B clade is one of the two early clades of plant PKSs that emerged before the divergence of Bryophytes and Tracheophytes, as shown by a kingdom-wide evolution analysis of plant PKSs (Naake *et al.*, 2021). TKPR1s and TKPR2s, on the other hand, form two clades of plant SDR superfamily enzymes. They belong to the SDR108E subfamily that harbors many plant secondary metabolite biosynthesis associated reductases, like the dihydroflavonol 4-reductase and anthocyanidin reductase in flavonoid biosynthesis, and cinnamoyl-CoA reductase in lignin biosynthesis (Moummou *et al.*, 2012). In evolution, TKPR2 appeared later than TKPR1, but earlier than many defense-related polyketide biosynthesis associated reductases (Moummou *et al.*, 2012), which supports the possibility that TKPR2 has been recruited from the ancient sporopollenin biosynthesis pathway to other PKS pathways not only in gerbera, but maybe also in other plants (Zhu *et al.*, 2021). Our data show how plants recruit conserved genes to perform new functions

within secondary metabolism, contributing to their environmental adaptation. This is evolution in front of our eyes.

Author contributions

LZ and THT designed the research; LZ, MP, JK and AT carried out the experiments; LZ and THT analyzed the results; LZ, THT and PE wrote the manuscript with input from all authors. All authors read and approved the final manuscript.

ORCID

Paula Elomaa https://orcid.org/0000-0001-6512-0810
Milla Pietiäinen https://orcid.org/0000-0002-4875-0682
Teemu H. Teeri https://orcid.org/0000-0002-3812-7213
Lingping Zhu https://orcid.org/0000-0001-6959-7755

Data availability

The nucleotide sequences of *GRED1* and *GRED2* have been deposited to GenBank with accession numbers MW842919 and MW842920, respectively.

References

Abe I. 2020. Biosynthesis of medicinally important plant metabolites by unusual type III polyketide synthases. *Journal of Natural Medicines* 74: 639–646.

Ainasoja MM, Pohjala LL, Tammela PS, Somervuo PJ, Vuorela PM, Teeri TH. 2008. Comparison of transgenic *Gerbera hybrida* lines and traditional varieties shows no differences in cytotoxicity or metabolic fingerprints. *Transgenic Research* 17: 793–803.

Austin MB, Noel JP. 2003. The chalcone synthase superfamily of type III polyketide synthases. *Natural Product Reports* 20: 79–110.

Bashandy H, Jalkanen S, Teeri TH. 2015. Within leaf variation is the largest source of variation in agroinfiltration of *Nicotiana benthamiana*. *Plant Methods* 11: 1–7.

Bisht R, Bhattacharyya A, Shrivastava A, Saxena P. 2021. An overview of the medicinally important plant type III PKS derived polyketides. *Frontiers in Plant Science* 12: 2155.

Bomati EK, Austin MB, Bowman ME, Dixon RA, Noel JP. 2005. Structural elucidation of chalcone reductase and implications for deoxychalcone biosynthesis. *Journal of Biological Chemistry* 280: 30496–30503.

Campuzano LDG, Shoolingin-Jordan PM. 1998. Incubation of 6-methylsalicylic acid synthase with alternative starter units in the absence of NADPH and the identification of the resulting triaceticacid lactones. *Biochemical Society Transactions* 26: S284.

Chang S, Puryear J, Cairney J. 1993. A simple and efficient method for isolating RNA from pine trees. *Plant Molecular Biology Reporter* 11: 113–116.

Deblaere R, Bytebier B, De Greve H, Deboeck F, Schell J, Van Montagu M, Leemans J. 1985. Efficient octopine Ti plasmid-derived vectors for *Agrobacterium*-mediated gene transfer to plants. *Nucleic Acids Research* 13: 4777–4788.

Deng X, Bashandy H, Ainasoja M, Kontturi J, Pietiäinen M, Laitinen RAE, Albert VA, Valkonen JPT, Elomaa P, Teeri TH. 2014. Functional diversification of duplicated chalcone synthase genes in anthocyanin biosynthesis of *Gerbera hybrida*. *New Phytologist* 201: 1469–1483.

Eckermann S, Schröder G, Schmidt J, Strack D, Edrada RA, Helariutta Y, Elomaa P, Kotilainen M, Kilpeläinen I, Proksch P. 1998. New pathway to polyketides in plants. *Nature* 396: 387–389.

Elomaa P, Teeri TH. 2001. Transgenic *Gerbera*. In: Bajaj YPS, ed. *Biotechnology in agriculture and forestry, vol. 48*. Berlin, Germany: Springer-Verlag, 139–154.

Fischbach MA, Walsh CT. 2006. Assembly-line enzymology for polyketide and nonribosomal peptide antibiotics: logic machinery, and mechanisms. *Chemical Reviews* 106: 3468–3496.

Gagne SJ, Stout JM, Liu E, Boubakir Z, Clark SM, Page JE. 2012. Identification of olivetolic acid cyclase from *Cannabis sativa* reveals a unique catalytic route to plant polyketides. *Proceedings of the National Academy of Sciences, USA* 109: 12811–12816.

Grienenberger E, Kim SS, Lallemand B, Geoffroy P, Heintz D, de Azevedo SC, Heitz T, Douglas CJ, Legrand M. 2010. Analysis of *TETRAKETIDE α-PYRONE REDUCTASE* function in *Arabidopsis thaliana* reveals a previously unknown, but conserved, biochemical pathway in sporopollenin monomer biosynthesis. *Plant Cell* 22: 4067–4083.

Hadfield AT, Limpkin C, Teartasin W, Simpson TJ, Crosby J, Crump MP. 2004. The crystal structure of the actIII actinorhodin polyketide reductase: proposed mechanism for ACP and polyketide binding. *Structure* 12: 1865–1875.

He F, Wang M, Gao M, Zhao M, Bai Y, Zhao C. 2014. Chemical composition and biological activities of *Gerbera anandria*. *Molecules* 19: 4046–4057.

Helariutta Y, Elomaa P, Kotilainen M, Seppänen P, Teeri TH. 1993. Cloning of cDNA coding for dihydroflavonol-4-reductase (DFR) and characterization of *dfr* expression in the corollas of *Gerbera hybrida* var. Regina (Compositae). *Plant Molecular Biology* 22: 183–193.

Helariutta Y, Kotilainen M, Elomaa P, Kalkkinen N, Bremer K, Teeri TH, Albert VA. 1996. Duplication and functional divergence in the chalcone synthase gene family of Asteraceae: evolution with substrate change and catalytic simplification. *Proceedings of the National Academy of Sciences, USA* 93: 9033–9038.

Hertweck C. 2009. The biosynthetic logic of polyketide diversity. *Angewandte Chemie International Edition* 48: 4688–4716.

Jenke-Kodama H, Müller R, Dittmann E. 2008. Evolutionary mechanisms underlying secondary metabolite diversity. *Progress in Drug Research* 65: 120–140.

Jindaprasert A, Springob K, Schmidt J, De-Eknamkul W, Kutchan TM. 2008. Pyrone polyketides synthesized by a type III polyketide synthase from *Drosophyllum lusitanicum*. *Phytochemistry* 69: 3043–3053.

Karimi M, Inzé D, Depicker A. 2002. GATEWAY™ vectors for *Agrobacterium*-mediated plant transformation. *Trends in Plant Science* 7: 193–195.

Katzen F. 2007. Gateway® recombinational cloning: a biological operating system. *Expert Opinion on Drug Discovery* 2: 571–589.

Kim SS, Douglas CJ. 2013. Sporopollenin monomer biosynthesis in arabidopsis. *Journal of Plant Biology* 56: 1–6.

Kim SS, Grienenberger E, Lallemand B, Colpitts CC, Kim SY, de Azevedo SC, Geoffroy P, Heintz D, Krahn D, Kaiser M *et al.* 2010. *LAP6/POLYKETIDE SYNTHASE A* and *LAP5/POLYKETIDE SYNTHASE B* encode hydroxyalkyl α-pyrone synthases required for pollen development and sporopollenin biosynthesis in *Arabidopsis thaliana*. *Plant Cell* 22: 4045–4066.

Koeduka T, Watanabe B, Suzuki S, Hiratake J, Mano J, Yazaki K. 2011. Characterization of raspberry ketone/zingerone synthase, catalyzing the alpha, beta-hydrogenation of phenylbutenones in raspberry fruits. *Biochemical and Biophysical Research Communications* 1: 104–108.

Kontturi J, Osama R, Deng X, Bashandy H, Albert VA, Teeri TH. 2017. Functional characterization and expression of GASCL1 and GASCL2, two anther-specific chalcone synthase like enzymes from *Gerbera hybrida*. *Phytochemistry* 134: 38–45.

Koskela S, Söderholm PP, Ainasoja M, Wennberg T, Klika KD, Ovcharenko VV, Kylänlahti I, Auerma T, Yli-Kauhaluoma J, Pihlaja K. 2011. Polyketide derivatives active against *Botrytis cinerea* in *Gerbera hybrida*. *Planta* 233: 37–48.

Kurosaki F, Mitsuma S, Arisawa M. 2002. Activation of acyl condensation reaction of monomeric 6-hydroxymellein synthase, a multifunctional polyketide biosynthetic enzyme, by free coenzyme A. *Phytochemistry* 61: 597–604.

Laitinen RAE, Immanen J, Auvinen P, Rudd S, Alatalo E, Paulin L, Ainasoja M, Kotilainen M, Koskela S, Teeri TH *et al.* 2005. Analysis of the floral transcriptome uncovers new regulators of organ determination and gene families related to flower organ differentiation in *Gerbera hybrida* (Asteraceae). *Genome Research* 15: 475–486.

Light RJ, Harris TM, Harris CM. 1966. Metabolism of triacetic acid and triacetic acid lactone. *Biochemistry* 5: 4037–4043.

Lim YP, Go MK, Yew WS. 2016. Exploiting the biosynthetic potential of type III polyketide synthases. *Molecules* 21: 806.

Livak KJ, Schmittgen TD. 2001. Analysis of relative gene expression data using real-time quantitative PCR and the $2^{-\Delta\Delta CT}$ method. *Methods* 25: 402–408.

Mascellani A, Leiss K, Bac-Molenaar J, Malanik M, Marsik P, Hernandez OE, Tauchen J, Kloucek P, Smejkal K, Havlik J. 2021. Polyketide derivatives in the resistance of *Gerbera hybrida* to powdery mildew. *Frontiers in Plant Science* 12: 790907.

Moghe GD, Last RL. 2015. Something old, something new: conserved enzymes and the evolution of novelty in plant specialized metabolism. *Plant Physiology* 169: 1512–1523.

Morita H, Wong CP, Abe I. 2019. How structural subtleties lead to molecular diversity for the type III polyketide synthases. *Journal of Biological Chemistry* 294: 15121–15136.

Moummou H, Kallberg Y, Tonfack LB, Persson B, van der Rest B. 2012. The plant short-chain dehydrogenase (SDR) superfamily: genome-wide inventory and diversification patterns. *BMC Plant Biology* 12: 1–17.

Murray RDH. 1997. Naturally occurring plant coumarins. In: Herz W, Kirby GW, Moore RE, Steglich W, Tamm C, eds. *Progress in the chemistry of organic natural products*. New York, NY, USA: Springer, 1–199.

Naake T, Maeda HA, Proost S, Tohge T, Fernie AR. 2021. Kingdom-wide analysis of the evolution of the plant type III polyketide synthase superfamily. *Plant Physiology* 185: 857–875.

Nagumo S, Toyonaga T, Inoue T, Nagai M. 1989. New glucosides of a 4-hydroxy-5-methylcoumarin and a dihydro-α-pyrone from *Gerbera jamesonii hybrida*. *Chemial and Pharmaceutical Bulletin* 37: 2621–2623.

Neves RPP, Ferreira P, Medina FE, Paiva P, Sousa JPM, Viegas MF, Fernandes PA, Ramos MJ. 2021. Engineering of PKS megaenzymes – a promising way to biosynthesize high-value active molecules. *Topics in Catalysis* 2021: 1–19.

Pietiäinen M, Kontturi J, Paasela T, Deng X, Ainasoja M, Nyberg P, Hotti H, Teeri TH. 2016. Two polyketide synthases are necessary for 4-hydroxy-5-methylcoumarin biosynthesis in *Gerbera hybrida*. *The Plant Journal* 87: 548–558.

Quilichini TD, Grienenberger E, Douglas CJ. 2015. The biosynthesis, composition and assembly of the outer pollen wall: a tough case to crack. *Phytochemistry* 113: 170–182.

Ruokolainen S, Ng YP, Broholm SK, Albert VA, Elomaa P, Teeri TH. 2010. Characterization of *SQUAMOSA*-like genes in *Gerbera hybrida*, including one involved in reproductive transition. *BMC Plant Biology* 10: 1–11.

Sainsbury F, Thuenemann EC, Lomonossoff GP. 2009. pEAQ: versatile expression vectors for easy and quick transient expression of heterologous proteins in plants. *Plant Biotechnology Journal* 7: 682–693.

Scott AI, Beadling LC, Georgopapadakou NH, Subbarayan CR. 1974. Biosynthesis of polyketides. Purification and inhibition studies of 6-methylsalicylic acid synthase. *Bioorganic Chemistry* 3: 238–248.

Shimizu Y, Ogata H, Goto S. 2017. Type III polyketide synthases: functional classification and phylogenomics. *Chembiochem* 18: 50–65.

Springob K, Samappito S, Jindaprasert A, Schmidt J, Page JE, De-Eknamkul W, Kutchan TM. 2007. A polyketide synthase of *Plumbago indica* that catalyzes the formation of hexaketide pyrones. *The FEBS Journal* 274: 406–417.

Stewart C Jr, Vickery CR, Burkart MD, Noel JP. 2013. Confluence of structural and chemical biology: plant polyketide synthases as biocatalysts for a bio-based future. *Current Opinion in Plant Biology* 16: 365–372.

Wallace S, Fleming A, Wellman CH, Beerling DJ. 2011. Evolutionary development of the plant spore and pollen wall. *AoB PLANTS* 11: 27.

Weng JK, Philippe RN, Noel JP. 2012. The rise of chemodiversity in plants. *Science* 336: 1667–1670.

Xie L, Liu P, Zhu Z, Zhang S, Zhang S, Li F, Zhang H, Li G, Wei Y, Sun R. 2016. Phylogeny and expression analyses reveal important roles for plant PKS III family during the conquest of land by plants and angiosperm diversification. *Frontiers in Plant Science* 7: 1312.

Yonekura-Sakakibara K, Higashi Y, Nakabayashi R. 2019. The origin and evolution of plant flavonoid metabolism. *Frontiers in Plant Science* 10: 943.

Yrjönen T, Vuorela P, Klika KD, Pihlaja K, Teeri TH, Vuorela H. 2002. Application of centrifugal force to the extraction and separation of parasorboside and gerberin from *Gerbera hybrida*. *Phytochemical Analysis* 13: 349–353.

Zhu L, Zhang T, Teeri TH. 2021. Tetraketide α-pyrone reductases in sporopollenin synthesis pathway in *Gerbera hybrida*: diversification of the minor function. *Horticulture Research* 8: 207.

Supporting Information

Additional Supporting Information may be found online in the Supporting Information section at the end of the article.

Fig. S1 Melting curves for quantitative polymerase chain reaction products.

Fig. S2 Reduction of methyl 3,5-dioxohexanoate by GRED1 and GRED2.

Table S1 Primer sequences used in this study.

Please note: Wiley Blackwell are not responsible for the content or functionality of any Supporting Information supplied by the authors. Any queries (other than missing material) should be directed to the *New Phytologist* Central Office.